# Performance of large homogeneous earth dams during strong ground motions

## Performance des grands barrages en terre homogène lors de forts mouvements de sol

Luca Masini, Sebastiano Rampello
*Dept. of Structural and Geotechnical Engineering, "Sapienza" University of Rome, Italy, luca.masini@uniroma1.it*

ABSTRACT: This paper discusses some aspects of the seismic behaviour of large homogeneous earth dams. Numerical analyses were carried out using a plane-strain finite difference model of an existing dam that has been calibrated using the monitoring data taken during the construction and the impoundment stages. The seismic performance of the dam was evaluated through a series of nonlinear dynamic analyses carried out in the time-domain using four real seismic records applied at the base of the model. The selected input motions are characterised by the same energy content and by a very high return period. Both the horizontal and the vertical component of the seismic action were applied at the base of the grid. In calculations, cyclic excess pore water pressure build-up was accounted for using the Finn-Byrne model. The seismic response of the dam is discussed showing the effects of input motion characteristics and of excess pore water pressure induced by earthquake loading on the maximum permanent settlement developed at the crest, that may be seen as an index of the seismic performance of the dam.

RÉSUMÉ: Cet article traite une partie des aspects du comportement sismique des grands barrages en terre homogène. Des analyses numériques ont été réalisées à l'aide d'un modèle de déformation plane aux différences finies d'une digue existante. Ce modèle a été étalonné en utilisant les données de surveillance recueillies lors des étapes de construction et d'endiguement. La performance séismique du barrage a été évaluée par une série d'analyses dynamiques non linéaires effectuées dans le domaine temporel à l'aide de quatre enregistrements sismiques réels appliqués à la base du modèle. Les mouvements d'entrée sélectionnés sont caractérisés par la même teneur énergétique et par une très élevée période de récurrence. Tous les deux composantes de l'action sismique, horizontale et verticale, ont été appliquées à la base de la grille. Au fin d'utiliser le modèle de Finn-Byrne, l'accumulation de la pression d'eau interstitielles de surpressions cyclique a été comptabilisée dans les calculs. La réponse sismique du barrage est discutée en montrant les effets des caractéristiques du mouvement d'entrée et les effets de la pression de l'eau d'excès des pores induite par le chargement du tremblement de terre de sur l'œuvre permanente maximale développée sur la crête, qui peuvent être considérés comme un indice de la performance sismique du barrage.

KEYWORDS: homogeneous earth dam, dynamic numerical analysis, cyclic excess pore water pressure, seismic performance.

## 1 INTRODUCTION

Seismic vulnerability of large earth dams existing in the Italian territory represents one of the most serious hazard of the Country in that a large number of them was designed without accounting for seismic loads explicitly. Hence, it is necessary to investigate the response of such structures when subjected to severe earthquake loading. This represents a complex task because of the transient nature of the earthquake loading that induces inertial forces and internal states that change with time. Moreover, excess pore water pressure may build-up in the saturated portion of the dam during cyclic loading, leading to a reduction of soil shear strength.

The seismic response of earth dams can be studied using different methods of analysis although classical procedures of analysis, such as the simple pseudo-static approaches, or the Newmark's type, sliding-block methods can only account for a few of the above mentioned factors, since are both based on a number of simplifying assumptions. Dynamic non-linear numerical analyses can instead account for an accurate description of actual dam geometry and hydraulic conditions, and can provide a more realistic description of the coupled hydro-mechanical soil behaviour during dynamic loads, through the use of constitutive models of varying degree of complexity, provided that the numerical model is calibrated correctly.

Therefore, reliable predictions of the seismic performance of earth dams require: a robust soil model; a detailed site characterisation for calibration of the numerical model; and accurate choice and description of the seismic input. Provided that an appropriate soil model is used and an accurate calibration is carried out, the evaluation of the seismic performance of a dam may change in a large span depending on the criteria adopted to select the seismic input and the assumption adopted in the analyses to reproduce the seismic action. Masini *et al.* (2016) and Han *et al.* (2016), among others, showed for example that neglecting the vertical component of the seismic motion may result in a substantial underestimate of the permanent settlements induced by the seismic event: the values obtained by applying a two-component input motion may be 1.5÷2 times higher than those computed using the horizontal component only of the motion. Conversely, the assumption of rigid bedrock, often adopted in the numerical analyses, may lead to excessively conservative results, with permanent settlements at the crest of the dam about twice higher those computed assuming the bedrock be compliant (Masini *et al.*, 2016).

This paper discusses some aspects of the seismic performance of large homogeneous earth dams. Numerical analyses were carried out with the finite difference code FLAC v.7 (Itasca 2011) using a numerical model that was conceived adopting some simplifying assumptions about the geometry of an existing homogeneous earth dam. This specific dam dikes the course of the Marana Capacciotti stream in Southern Italy and represents a well documented case-history (Calabresi et al. 2000, Cascone and Rampello 2003, Amorosi and Elia 2008, Rampello et al. 2009, Elia et al. 2010), with a comprehensive geotechnical characterisation for the embankment and the foundation soils and monitoring data available for both the construction and the impounding stages.

The seismic response of the dam was investigated through time-domain dynamic analyses in which the input ground motion applied at the base of the model was represented by real

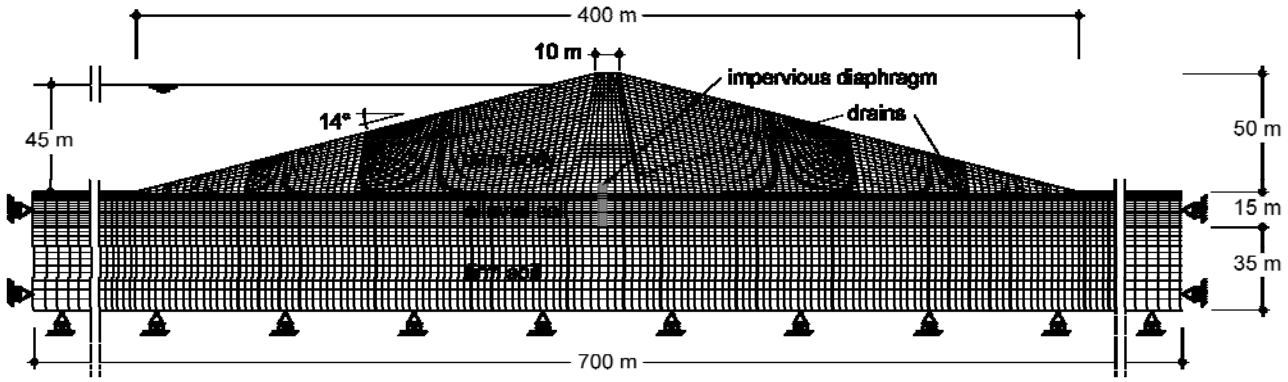


Figure 1. Finite difference grid adopted in the analyses

Table 1. Mechanical soil properties

| soil | γ (kN/m³) | c' (kPa) | φ' (°) | $k_0$ (-) | $k$ (m/s) | $A$ (MPa) | $B$ (MPa) | $n$ (-) | ν (-) |
|---|---|---|---|---|---|---|---|---|---|
| dam body | 20.8 | 20 | 28 | - | $10^{-7}$ | 19.48 | 1573 | 0.75 | 0.30 |
| foundation soil | 20.4 | 7 | 32 | 1.5 | $10^{-6}$ | 19.48 | 2155 | 0.73 | 0.32 |
| firm soil | 20.6 | - | - | 1.5 | $10^{-9}$ | 2060 | 0 | - | 0.32 |

time histories of shear and normal stresses, to account for bedrock compliance. In the analyses, both the cyclic soil behaviour and the excess pore water pressure build up were simulated.

The influence of the input motion was studied by applying four real seismic records characterized by the same energy content but different values of frequency content and significant duration. It can be anticipated that seismic records characterised by a longer duration and with a frequency content closer to the fundamental frequency of the system will induce larger deformations in the dam. Notwithstanding, selection of the input motion is often simply based on compatibility of seismic motions with the design elastic response spectra prescribed by national or international guidelines or building codes.

The analyses were also repeated inhibiting the development of excess pore water pressure, to evaluate the influence of the coupled hydro-mechanical soil behaviour on the seismic performance of the dam.

## 2 FINITE DIFFERENCE MODEL

The main cross section of the Marana Capacciotti was converted into a simplified plane-strain numerical model. Figure 1 shows the mesh adopted for the analyses. The dam has a height H = 50 m, a width of 400 m at the base and the slope of the flanks is $\alpha = 14°$. The finite difference mesh extends horizontally to 350 m from the dam axis and vertically down to a depth of 50 m. The embankment is mainly formed by sandy silt and clay. The foundation soil consists of two layers: an alluvial soil deposit, 15 m thick, made of medium-stiff silt and clay, and a stiff silty-clay deposit which extends down to the deep bedrock formation. A detailed description of the geotechnical characterisation at the site of Marana Capacciotti dam is given by Calabresi *et al.* (2000) and Cascone and Rampello (2003). The drainage system of the embankment consists of a sub-vertical central drain and a horizontal drain located at the toe of the downstream slope. An impervious diaphragm extending into the lower firm soil prevents seepage through the alluvial deposit underlying the dam.

The numerical analyses were carried out in terms of effective stresses using the finite difference code FLAC v.7. The embankment soil and the alluvial layer were modelled as elastic-perfectly plastic materials with Mohr-Coulomb's failure criterion and zero dilatancy. The strength and stiffness parameters of the soils were obtained from the geotechnical investigations carried out throughout the earth dam and in the foundation soils (Calabresi *et al.*, 2000). Table 1 lists the shear strength parameters obtained from standard consolidated undrained triaxial compression tests and drained direct shear tests. The small-strain shear modulus $G_0$ was expressed as a function of the mean effective stress $p'$:

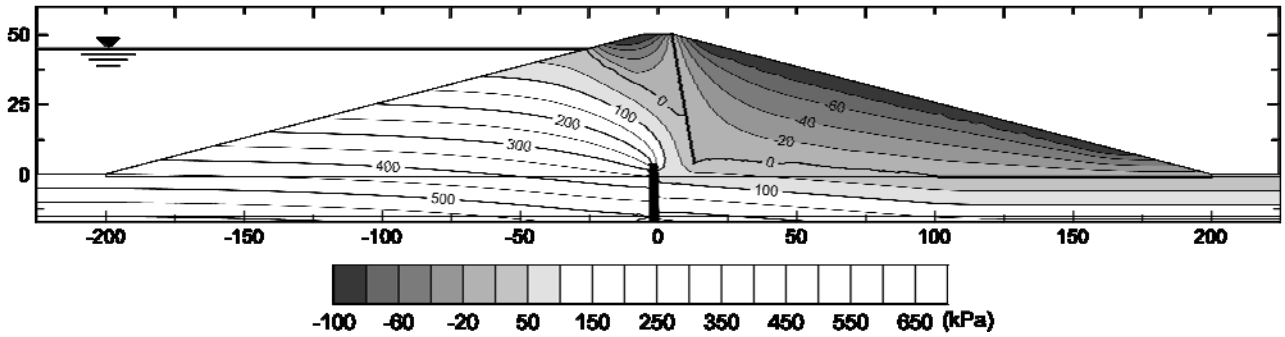


Figure 2. Contour lines of the steady-state pore water pressure computed at the maximum reservoir level

$$G_0 = A + B \cdot \left( \frac{p'}{p_{ref}} \right)^n \quad (1)$$

where $p_{ref}$ = 1 kPa is a reference pressure. Values of coefficients $A$, $B$, and $n$ were selected to match the measurements of $G_0$ obtained from resonant column tests carried out on undisturbed samples retrieved from the dam body and the foundation soil. The stiff clay deposit found underneath the alluvial layer was regarded as a bedrock characterised by a shear wave velocity $V_s$ = 1000 m/s, with constant values of small-train shear modulus $G_0$ = 2060 MPa and bulk modulus $K$ = 5026.4 MPa.

The initial state of effective stress prior to the dynamic calculation phase was computed simulating the static staged construction of the dam, assumed as a drained process, and the impoundment stage; the operative values of shear stiffness adopted in the static calculations were calibrated to reproduce the settlement profiles observed at the end of construction. Specifically, an operative shear modulus equal to about 5% of $G_0$ was used for the dam body and the foundation soil, while 8% of $G_0$ was used for the bedrock. At the end of each calculation phase, the soil stiffness was updated to correspond to the new effective stress state. The impounding of the reservoir and the associated steady-state seepage flow through the dam were simulated by raising the water level in three stages of 15 m, reaching the maximum storage level of 45 m. During the steady-state seepage calculation, negative values of pore water pressure $u$ were allowed to develop by gradually reducing the permeability of the portion of the dam located above the "free surface" defined by the condition $u$ = 0, thus confining the hydraulic flow below it while keeping the whole embankment saturated. Figure 2 shows the contour lines of the pore water pressure resulting from the steady-state seepage flow at the maximum storage level. A threshold value of -100 kPa was adopted to limit negative pore water pressure.

## 3 DYNAMIC ANALYSIS

Starting from the end-of-construction stage, time-domain dynamic analyses were carried out by applying time-histories of the input motion to the bottom boundary of the grid. FLAC "free-field" boundary conditions were activated to the lateral sides of the grid, while "quiet" (viscous) boundary conditions were applied at the base; the initial soil stiffness was set equal to the small strain shear stiffness.

Table 2. Properties of the input seismic records

| | Record | $F$ | $a_{max}$ (g) | $I_a$ (m/s) | $T_m$ (s) | $D_{5\text{-}95}$ (s) |
|---|---|---|---|---|---|---|
| (A) | Tolmezzo NS | 1.8 | 0.64 | 2.56 | 0.40 | 4.31 |
| | Tolmezzo V | 1.8 | 0.48 | 1.08 | 0.21 | 5.16 |
| (B) | Nocera Umbra | 1.0 | 0.59 | 2.80 | 0.23 | 5.01 |
| | Nocera Umbra Z | 1.0 | 0.39 | 0.71 | 0.33 | 3.98 |
| (C) | Landers CLW LN | 1.5 | 0.44 | 2.57 | 0.42 | 10.39 |
| | Landers CLW UP | 1.5 | 0.25 | 1.39 | 0.23 | 17.12 |
| (D) | Kobe TAZ000 | 0.9 | 0.63 | 2.56 | 0.80 | 4.6 |
| | Kobe TAZUP | 0.9 | 0.38 | 0.87 | 0.50 | 2.2 |

The cyclic behaviour of the dam body and the foundation soil was described through the hysteretic damping model Sigmoidal4, implemented in FLAC. The model requires definition of the small-strain shear stiffness $G_0$ and of a backbone curve: $G_0$ was expressed as a function of the mean effective stress (see Eq. 1), while the backbone curve was calibrated to reproduce the modulus decay curves obtained from resonant column tests, as described by Masini *et al.* (2016). A small amount of Rayleigh damping was also introduced in the analyses to attenuate the soil response at very small strains and to reduce spurious high-frequency noise. Rayleigh's coefficients were calibrated to this purpose using the procedure proposed by Amorosi *et al.* (2010), in order to obtain a maximum damping of 1% in the range of frequencies defined by the first and the last value excited by the input motion.

To account for the eventual reduction in the shear strength of the earth dam, due to the excess pore pressure build-up in undrained conditions, the hysteretic and Mohr-Coulomb models

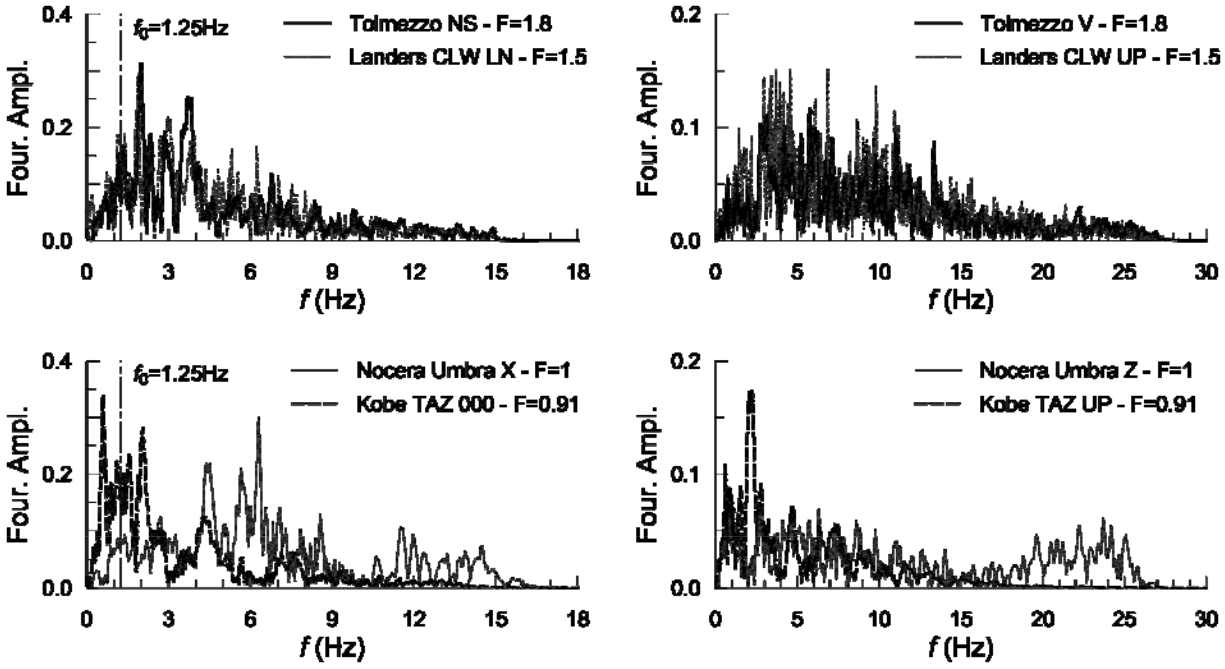


Figure 3. Amplitude Fourier spectra of the horizontal (left) and the vertical (right) components of the input motions

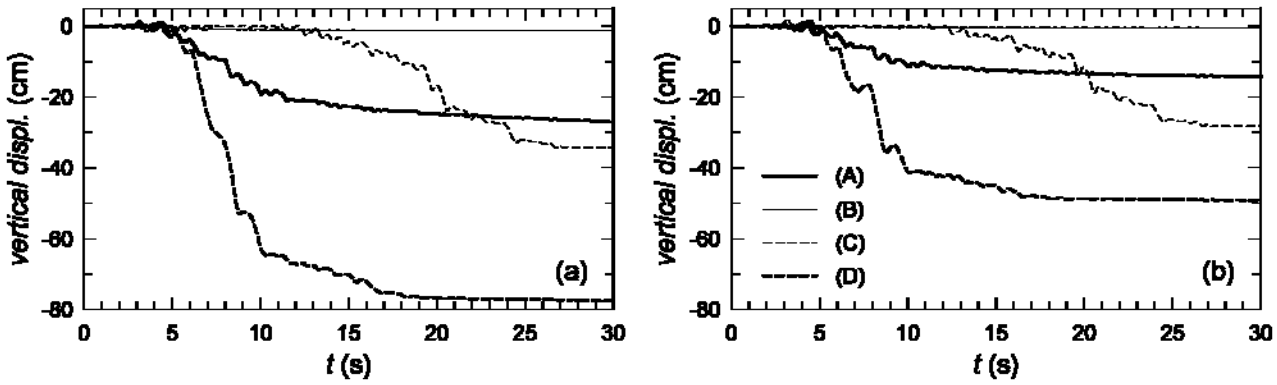


Figure 4. Settlements of the crest relative to the base of the dam, computed at its axis

were coupled with the Finn-Byrne model (Byrne, 1991), implemented in the FLAC code. In this model, the cyclic irreversible volume strain $\varepsilon_{vd}$ is expressed in an incremental form:

$$\Delta\varepsilon_{vd} = \gamma \cdot C_1 \exp\left(-C_2 \cdot \frac{\varepsilon_{vd}}{\gamma}\right) \quad (2)$$

where $\Delta\varepsilon_{vd}$ is the incremental volumetric strain, $\gamma$ is the cyclic shear-strain amplitude, $C_1$ e $C_2$ are two model constants. Assuming soil behaviour be elastic and loading conditions be undrained, the cyclic excess pore pressure is $\Delta u = K \cdot \varepsilon_{vd}$, where $K$ is the bulk modulus. The model allows for the development of excess pore water pressure until the stress state reach the yield surface. The Finn-Byrne constant values $C_1 = 0.035$ e $C_2 = 12$ were calibrated to reproduce the ratios $\Delta u/p'_0$ of excess pore water pressure to the mean effective stress observed in resonant column tests and reported in Rampello *et al.* (2009).

Four real seismic records were used as input motion, selected to be compatible with the seismicity of the site (Cascone and Rampello, 2003); three of them are characterised by similar durations but different frequency contents (Tolmezzo (A), Nocera Umbra (B) and Kobe (D) records), while the Landers record (C) has a frequency content similar to Tolmezzo record (A), but a duration about 2.4 times longer. In the analyses, both the horizontal and the vertical components of the acceleration records were multiplied by the same scaling factor $F$, to match the elastic response spectrum of the newly-released Italian building code for dams; in this study a return period $T_R = 2475$ years was assumed. Some properties of the selected records are reported in Table 2, where $a_{max}$ is the peak ground acceleration, $I_A$ is the Arias intensity, $D_{5\text{-}95}$ is the significant duration computed between 5% and 95% of the Arias Intensity, and $T_m$ is the mean quadratic period as defined by Rathje *et al.* (1998). Figure 3 shows the Fourier's amplitude spectra for the horizontal and the vertical components of the selected records. The North-South record of Tolmezzo station (Friuli 1976 earthquake), scaled by a factor $F = 1.8$, was taken as the reference input motion; to evaluate the effect of the ground motion characteristics on the seismic performance of the dam, two records were selected with similar Arias Intensity $I_A$ and significant duration $D_{5\text{-}95}$ but different mean period $T_m$: the Nocera Umbra record (Umbria-Marche 1997 earthquake) is characterized by a lower $T_m$, while the Takarazu record (Kobe 1995 earthquake) has a higher $T_m$ than the Tolmezzo one. Another record (Coolwater record, Landers 1992 earthquake) was also selected with values of Arias intensity $I_A$ and mean period $T_m$ similar to those of Tolmezzo record, but with a higher duration $D_{5\text{-}95}$. The analyses were carried out assuming a compliant bedrock, by applying a time history of shear stress $\tau_{xy}$ at the base of the model (Joyner and Chen, 1975):

$$\tau_{xy}(t) = \rho V_s \cdot \int a_x(t) \quad (3)$$

where $\rho = 2.06$ Mg/m$^3$ and $V_S = 1000$ m/s are the bedrock density and shear wave velocity, while $\int a_x(t)$ is the velocity obtained by integrating the horizontal component of the acceleration time history. Similarly, the vertical component of input motion is described by a time history of normal stress $\sigma_{yy}$:

$$\sigma_{yy}(t) = \rho V_p \cdot \int a_y(t) \quad (4)$$

where $V_p$ is the compression wave velocity at the bedrock, assumed equal to 1944 m/s, while $\int a_y(t)$ is the velocity obtained integrating the vertical component of the acceleration time history.

Undrained conditions were assumed in calculations, adopting a water bulk modulus $K_w = 1$ GPa.

Figure 4a shows the time histories of vertical displacements of the crest, computed at the centre line, relative to the base of the dam. Negative values refer to settlements. Tolmezzo record (A) is characterised by a frequency content about twice higher than the first natural frequency of the dam, equal to 1.24 Hz. The maximum relative settlement computed using this record is equal to 27 cm, that can be considered as representative of a satisfactory seismic performance of the dam during extreme loading conditions since the seismic action refers to a large return period ($T_R = 2475$ years). The Nocera Umbra record (B) is characterized by a frequency content about 3.5 times larger the first natural frequency of the dam and induces negligible settlements, lower than about 2 cm. Conversely, the mean period of Kobe TAZ 000 record (D), equal to $T_m = 0.802$ s, is very close to the fundamental period of the system ($T_0 = 0.806$ s). This record induces a relative settlement at the crest of the dam equal to 77 cm, which is about 3 times higher than the value computed using the Tolmezzo record. Finally, the Landers CLW record (C), that is characterized by about the same frequency content as Tolmezzo (A), but by has a duration about 2.4 times longer, results in a settlement increase of about 26 % (34 cm).

Figure 5a shows the deformed mesh computed at the end of Kobe TAZ000 record (D): large displacements develop in the upstream slope, from the toe to the crest, partially involving also the foundation soil. The stress state within the embankment was evaluated using the shear strength ratio $t/t_{max}$, where $t$ is the radius of the current Mohr's circle and $t_{max}$ is the radius of a Mohr's circle having the same centre $s'$, but tangent to the failure envelope; the shear strength of the soil is fully mobilised as the ratio $t/t_{max}$ approaches unity. Figure 5b shows the contour

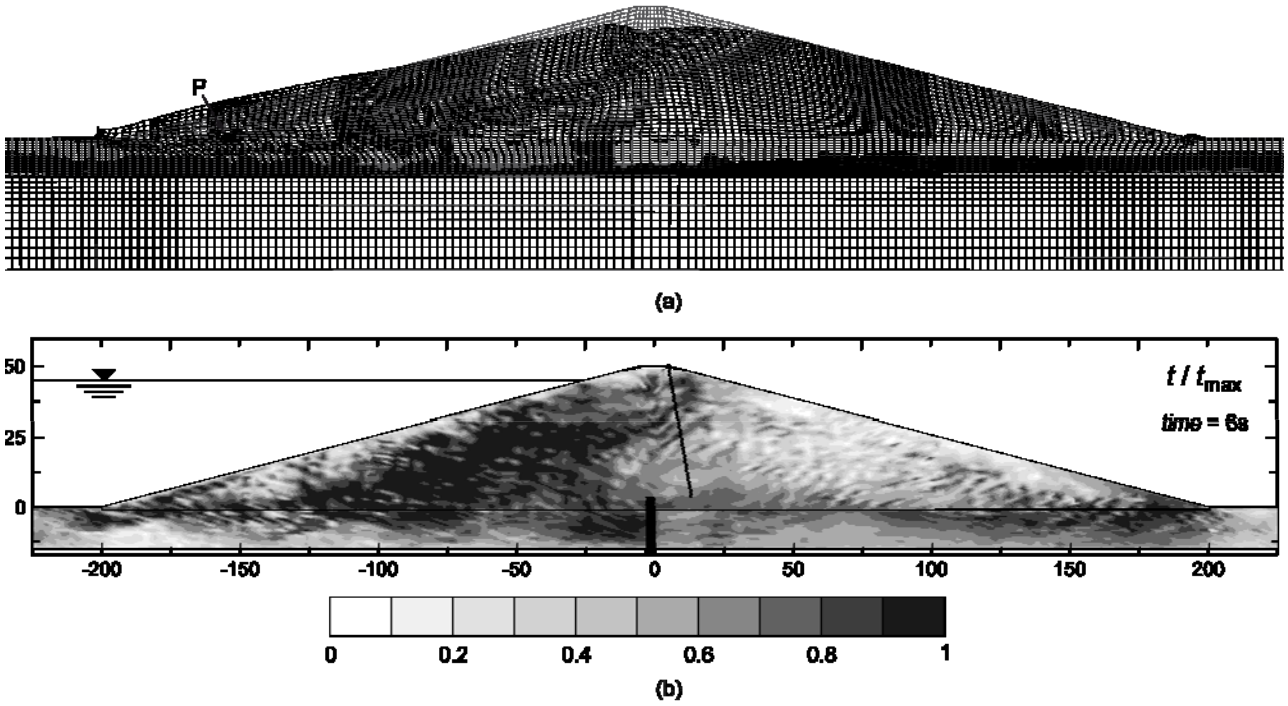


Figure 5. Analyses results for Kobe TAZ000 record (D): (a) deformed mesh computed at the end of ground motion (displacement scaling factor 1:10) and (b) contour lines of mobilised shear strength $t/t_{max}$ at a time instant during the strong motion phase.

lines of $t/t_{max}$ obtained using record D: at the time of the strong motion phase, when high shear strain increments were seen to develop ($t = 6$ s), values of $t/t_{max}$ close to unity were computed in a large portion of the upstream slope. Therefore, the deformation pattern depicted in Figure 5a is the result of transient mobilisation of soil strength during the seismic shaking, which induces the accumulation of permanent displacements. Similar deformation patterns were also observed for the other input motions, but with smaller values of permanent displacements. In any case, for all the considered input, the maximum settlement computed at the crest of the dam was smaller than the available freeboard, equal to 2.6 m.

The analyses were also repeated without accounting for pore water pressure build up. Figure 4b shows the relative settlements computed for the four seismic input. Much lower settlements were obtained for record A, C, D, with reductions of about 50, 20 and 40%, respectively, while negligible relative settlements were again computed using record B. The observed increase in dam displacements when positive excess pore water pressures are allowed to develop may be ascribed to the reduction in shear strength of the soil. In fact, the shear strength $q_f$ can be written as:

$$q_f = M \cdot p' = M \cdot \left[ \left( p_0 + \Delta p \right) - \left( u_0 + \Delta u \right) \right] = M \cdot \left[ p'_0 - \left( \Delta u - \Delta p \right) \right] = q_{f,0} - \Delta q_f \quad (5)$$

where $M$ identifies the Mohr-Coulomb criterion in the $p'$- $q$ plane and $\Delta q_f$ represents the reduction in shear strength related to pore water pressure build up during seismic shaking; $\Delta q_f$ increases with the difference between the change in pore water pressure and the change in total mean stress, $(\Delta u - \Delta p)$. This term is plotted in Figure 6 for a soil zone in the upstream slope (point P of Figure 5), where high rates of shear strain develop. Consistently with the displacement time histories, the maximum values of $(\Delta u - \Delta p)$ were obtained for record D, for which $(\Delta u - \Delta p) \approx 45$ kPa at the end of the ground motion. Lower values were computed for records A and C, while, for record B, the increase of the mean total stress $\Delta p$ was larger than the accumulated positive excess pore water pressure $\Delta u$.

## 4 CONCLUSIONS

The seismic performance of a large homogeneous earth dam was studied through a series of dynamic analyses in which the input seismic records were selected to satisfy compatibility with the design spectrum as required by the Italian building code. Reference to severe seismic events was made assuming a return period of 2475 years. As it could be anticipated, the largest settlements of the crest of the dam were computed when the mean period of the input motion was about equal to the first fundamental period of the system. Settlements also increase with the duration of the strong motion phase, though to a lower

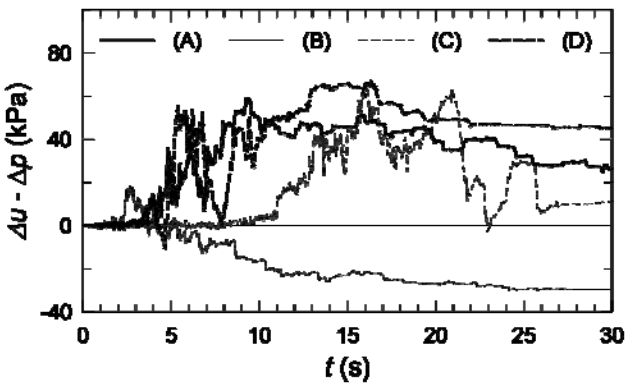


Figure 6. Difference between the changes in pore water pressure and total mean stress computed at the toe of the dam (element P), close to the upstream slope.

extent. Then, besides that meet compatibility criteria with the design elastic response spectrum, the seismic input should also be characterised by a frequency content similar to that of the system and have a long duration.

Calculations also showed that neglecting pore water pressure build up during seismic shaking may yield to substantial underestimate of dam settlements, as high as 50 %.

Anyway, despite the high return period of input motions considered in the analyses, this corresponding to a very severe seismic scenario, the maximum permanent settlements computed at the crest of the dam was always lower than the available freeboard, this indicating a satisfactory performance of the dam to intense earthquake loading.

## 5 ACKNOWLEDGEMENTS

The research work presented in this paper was partly funded by the Italian Department of Civil Protection under the ReLUIS 2014-2016 research project.

## 6 REFERENCES

Amorosi A. and Elia G. 2008. Analisi dinamica accoppiata della diga Marana Capacciotti. *Rivista Italiana di Geotecnica*, Patron editore, Bologna, 52 (4), 78-95.

Byrne P. 1991. A Cyclic Shear-Volume Coupling and Pore-Pressure Model for Sand. *Proc. Second International Conference on Recent Advances in Geotechnical Earthquake Engineering and Soil Dynamics*, St. Louis, Missouri, 47-55.

Calabresi G., Rampello S., Sciotti A., Amorosi A. 2000. *Diga sulla Marana Capacciotti: verifica delle condizioni di stabilità e analisi del comportamento in condizioni sismiche*. Res. Rep.: Università degli Studi di Roma La Sapienza, Dip. di Ingegneria Strutturale e Geotecnica. Bastogi Editrice, Foggia.

Cascone E. and Rampello S. 2003. Decoupled seismic analysis of an earth dam. *Soil Dynamics and Earthquake Engineering* 23 (5), 349-365.

Elia G., Amorosi A., Chan A.H.C., Kavvadas M.J. 2010. Fully coupled dynamic analysis of an earth dam. *Géotechnique* 61 (7), 549-563.

Han B, Zdravkovic L., Kontoe S., Taborda D.M.G. 2016. Numerical investigation of the response of the Yele rockfill dam during the 2008 Wenchuan earthquake. *Soil Dynamics and Earthquake Engineering* 88, 124-142.

Itasca 2011. FLAC Fast Lagrangian Analysis of Continua v. 7.0. User's Manual. Minneapolis, MN, USA: Itasca Consulting Group.

Joyner W.B. and Chen A.T.F. 1975. Calculation of Nonlinear Ground Response in Earthquakes. *Bulletin of the Seismological Society of America* 65 (5), 1315-1336.

Masini L., Rampello S., Callisto L. 2016. Seismic behaviour of large earth dams: from site investigations to numerical modelling. *Proc. 1st IMEKO TC-4 International Workshop on Metrology for Geotechnics*, Benevento, Italy, 288-294.

Rampello S., Cascone E., Grosso N. 2009. Evaluation of the seismic response of a homogeneous earth dam. *Soil Dynamics and Earthquake Engineering* 29 (5), 782-798.

Rathje E.M., Abrahamson N.A., Bray, J.D. 1998. Simplified frequency content estimates of earthquake ground motions. *J. Geotech. Geoenviron. Engng, ASCE* 124 (2), 150-159.